P.A. Politzer and J.S. Murray (Editors)
Energetic Materials, Part 1: Decomposition, Crystal and Molecular Properties
Theoretical and Computational Chemistry, Vol. 12

Chapter 2

Characterisation of explosive materials using molecular dynamics simulations

P. Čapková[a], M. Pospíšil[a], P. Vávra[b] and S. Zeman[b]

[a]Department of Chemical Physics and Optics, Faculty of Mathematics and Physics, Charles University Prague, Ke Karlovu 3, 12116 Prague 2, Czech Republic.

[b]Department of Theory and Technology of Explosives, University of Pardubice, 53210 Pardubice, Czech Republic.

1. INTRODUCTION

Classical molecular dynamics simulations of the unimolecular decomposition have been performed for selected molecules exhibiting different impact sensitivity and different detonation energy: (1) $(CH_2NNO_2)_3$, more commonly known as RDX, (2) $(CH_2NNO_2)_4$, known as HMX, (3) $(NH_2)_2CC(NO_2)_2$, known as DADNE and (4) $(NH_2)_2CNNO_2$, known as NQ. A potential energy was described using empirical force field. The analysis of dynamic trajectories enabled us to reveal step by step the mechanism of decomposition and to determine the parameters characterizing the impact sensitivity and explosives performance (detonation energy) of these energetic materials. This work is a continuation of previous studies focused to unraveling of molecular decomposition process in explosive materials, see Ref.1-10. We use the classical molecular dynamics in *Cerius*^{2} *(Materials Studio)* modeling environment, Ref. 11, for the simulation of molecular decomposition. The aim of the present work is to reveal step by step the mechanism of explosion and to find the way of reliable characterization of explosive materials using classical molecular dynamics simulations of the uni-molecular decomposition process. The structure of four molecules selected for dynamic simulations are reported in Ref. 12-15, for RDX, β-HMX, DADNE and NQ. Molecular structures are shown in the Fig. 1a-d.

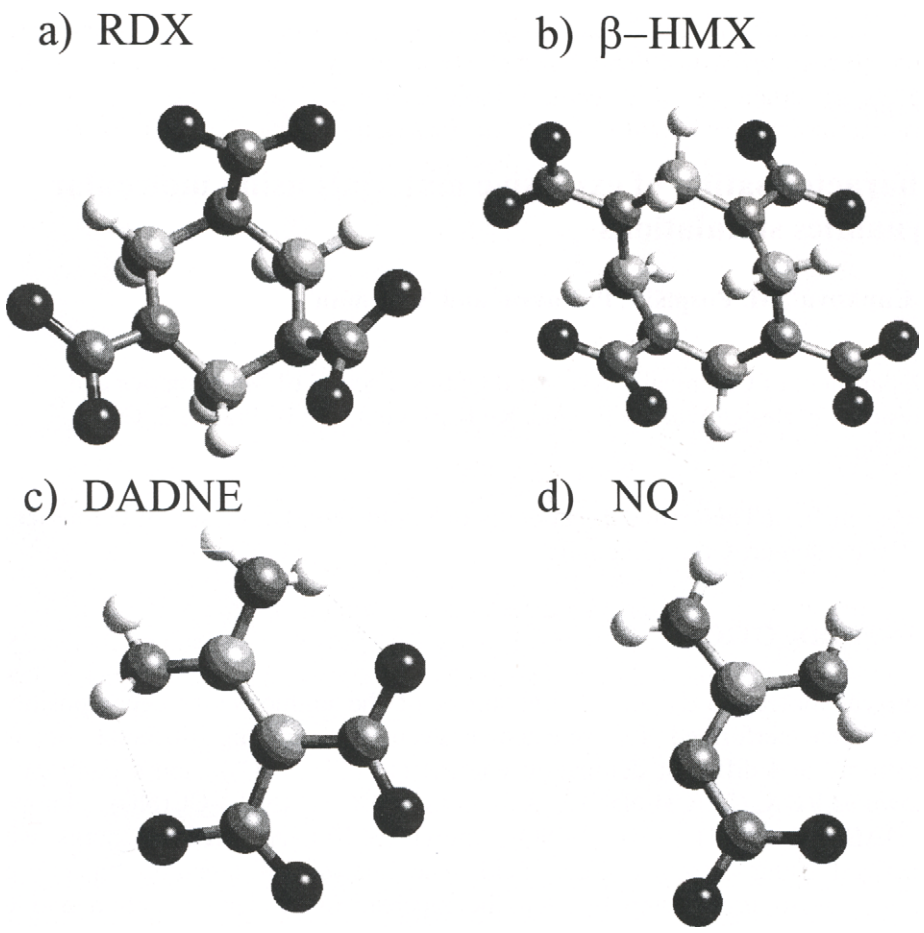

Fig. 1. Initial models of molecules for dynamic simulations:

a) RDX - cyclotrimethylene-trinitramine, $(CH_2NNO_2)_3$;

b) β-HMX - β-cyclotetramethylene-tetranitramine, $(CH_2NNO_2)_4$;

c) DADNE - 1,1-diamino-2,2-dinitroethylene, $(NH_2)_2CC(NO_2)_2$;

d) NQ - nitroguanidine, $(NH_2)_2CNNO_2$.

Impact sensitivities were studied using drop weight apparatus and were reported together with calculated detonation energy in Ref. 16. Comparing the molecular structures of a chosen molecules and their impact sensitivities characterized by the height *h,* i.e. the critical value of the fall height of the drop weight (see Table 1), we can divide these molecules into two groups:

1. I. group: molecules RDX and β–HMX with high sensitivity, i.e. with low *h* value ~24 cm and ~26 cm, see Table 1;
2. II. group: molecules DADNE and NQ with low impact sensitivity, i.e. *h* ~ 100 cm and ~177 cm., see Table 1.

Similarity in behavior of molecules belonging to the same group and the differences between groups I and II led us to investigate the decomposition process just for these four types of molecules using classical molecular dynamics simulations. Analyzing the molecular dynamics trajectories we will focus our attention to the following goals:

- To reveal the mechanism and kinetics of the decomposition process at the molecular scale;
- To derive the parameters characterizing the impact sensitivity;
- To derive the parameters characterizing the detonation energy.

Special attention will be paid to the investigation of two decomposition pathways for molecules RDX, which have been reported in previous studies Ref. 3,7,10 as R1 and R2

$$RDX \rightarrow C_3H_6N_5O_4 + NO_2 \quad (R1)$$
$$RDX \rightarrow 3CH_2NNO_2 \quad (R2)$$

In the reaction R1 the rupture of the first C-N bond is followed by the rupture of the first N-NO_2 bond (release of the nitrogroup), as one can see in the Fig. 2a. Then the rest of the molecule is gradually totally decomposed. Reaction R2 starts with the rupture of three C-N bonds and subsequent break up of the molecule into three CH_2NNO_2 fragments (see Fig. 2b). Afterwards the NO_2 groups are released from these fragments. Dynamics trajectory enables the animation of molecular motion with the time resolution 1fs and the visualization of the molecular decomposition process in real time.

2. STRATEGY OF MOLECULAR DYNAMICS SIMULATIONS

A natural starting point for a theoretical study is to investigate the chemical decomposition at the molecular scale. Classical molecular dynamics simulations in *Cerius*[2] *(Materials Studio)* modeling environment were carried out to calculate dynamics trajectory for one isolated molecule. Searching for the

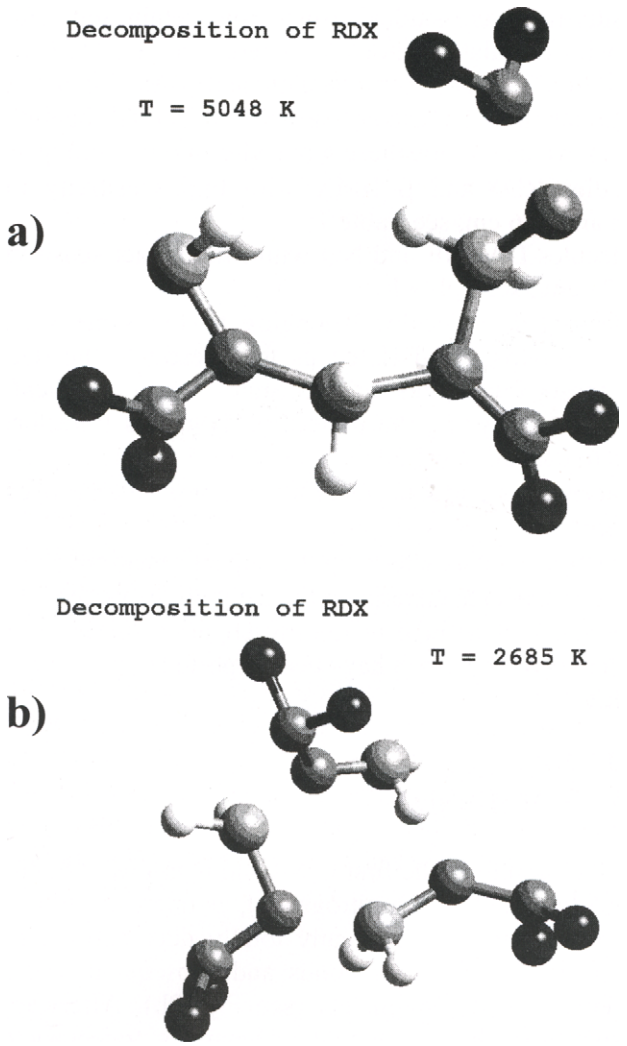

Fig. 2. Decomposition of RDX, snapshots extracted from dynamics trajectories:

a) Reaction R1 at temperature 5048 K;

b) Reaction R2 at temperature 2685 K.

optimum strategy we have found the following conditions for dynamics simulations:

- We used the "*Impulse dynamics*", that means at the beginning the system get the initial impulse, corresponding approximately to double of the chosen temperature to assign the initial velocities to the atoms using Maxwell-Boltzmann equation.
- The calculations were performed in *microcanonical ensemble* (NVE). Newtons equations of motion were integrated by using Verlet integrator. Although the temperature is not controlled during NVE dynamics, *Cerius*^{2} allows us to hold the temperature within specified tolerances by periodic rescaling of the velocities.
- Dynamics trajectories were calculated under following conditions: force field *cvff_950*, see Ref. 17, has been used with dynamics time step 0.001ps. The length of the dynamic trajectory in *ps*, the initial temperature and consequently the initial energy impulse were dependent on the sensitivity of a given molecule and have estimated as a result of dynamic simulations experiments. Atomic charges in *Cerius*^{2} are calculated using the charge equilibration method (Ref.18).
- Building the initial models we used the crystallographic conformation as a starting geometry for dynamic simulations.

As a result of dynamic simulations we obtained the dynamic trajectory file including the time dependence of the temperature, kinetic, potential and total energy and development of the decomposition process. The animation of the molecular motion during dynamic simulations enables us to visualize the time dependence of the uni-molecular decomposition process, starting from the first bond scission to the release of the nitro-groups NO_2. The course of dynamic trajectories, i.e. the time dependence of temperature, kinetic, potential and total energy allows us to estimate the parameters characterizing the explosives as to the sensitivity and performance.

3. RESULTS AND DISCUSSION

Analysis of dynamic trajectories revealed the mechanism of the molecular decomposition for selected molecules: RDX, β–HMX, DADNE and NQ. The time dependence of the kinetic energy for these molecules is in the Fig. 3-7. The course of dynamic trajectories showed the similar character of the decomposition process for molecules of the I.group i.e. RDX, and β–HMX. Molecules of the II.group - DADNE and NQ also exhibit similar features during decomposition process, however the character of the dynamic trajectories and

decomposition for DADNE and NQ is different from the I.group (RDX and β–HMX), as one can see comparing the Fig. 3-7. Analyzing dynamic trajectories we paid attention to the time, temperature and kinetic energy corresponding to the rupture of the first bond in the molecule and to the release of the first NO_2 group from the molecule. The initial temperature impulse assigned to the system in present dynamic simulations was set up as the temperature necessary for the start of decomposition process in time interval 0 – 100 ps. In general the use of lower temperature leads to a later start of decomposition, anyway the character of dynamic trajectories remains the same for a given molecule. The time corresponding to the start of decomposition (i.e. the moment when the first bond is definitely ruptured) is for given molecule affected by the temperature of the thermal bath. However the role of statistics should be taken into account. Therefore all the characteristic parameters derived from dynamic trajectories at certain temperature were averaged over 20 independent impulse dynamic trajectories.

3.1 Decomposition of RDX and β–HMX

Two decomposition processes suggested on the base of experiment by B.M. Rice et al. Ref. 7 and Shalashilin & Thompson Ref. 3, were confirmed by the analysis of dynamic trajectories for both molecules RDX and β–HMX. However our results of molecular dynamics simulations did not confirm the conclusion of Rice, see Ref. 7, that the reaction R1 (RDX $\rightarrow C_3H_6N_5O_4 + NO_2$) occurs at low temperatures and the reaction R2 (RDX $\rightarrow 3CH_2NNO_2$) is more probable at high temperatures. Analysis of 40 dynamic trajectories for RDX and β–HMX showed that both reactions occur at low and high temperatures with the same probability. Dynamic simulations show that most probable decomposition process is the combination of reaction R1 and R2. In such a case the first NO_2 group is released neither after first C-N bond rupture (R1), nor after all C-N bond rupture (R2), but after the second (in case of β–HMX second or third) C-N bond rupture according to the scheme: C-N $\rightarrow$ C-N $\rightarrow$ C-N $\rightarrow$ N-NO_2 $\rightarrow$ C-N.

Two examples of the dynamic trajectories (the time dependence of the kinetic energy) for the molecule RDX are presented in the Fig. 3 and 4, where the Fig. 3 illustrates the reaction pathway R1 and the Fig. 4 shows the trajectory for the reaction R2. Arrows mark the points on the dynamic trajectory corresponding to the rupture of C-N and N-NO_2 bonds. Fig. 5 shows the example of trajectory for β–HMX, where the decomposition process is the combination of R1 and R2 reactions. Anyway the character of dynamic trajectories and consequently the character of molecular decomposition is very similar for RDX and β–HMX.

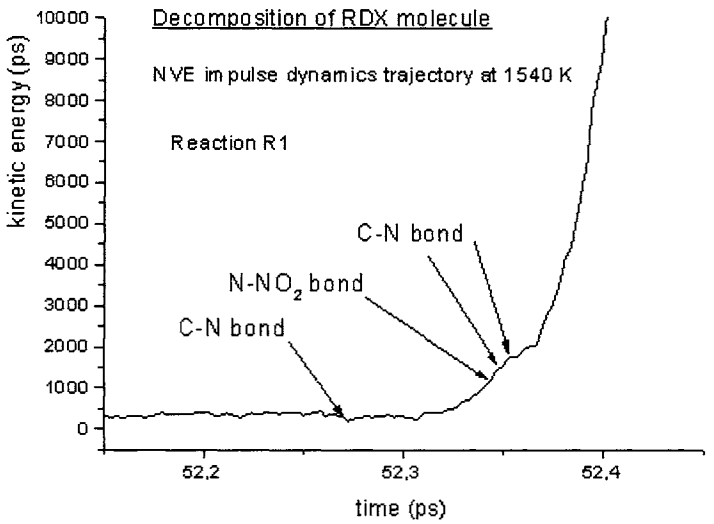

Fig.3. Impulse dynamics trajectory for RDX , reaction R1.

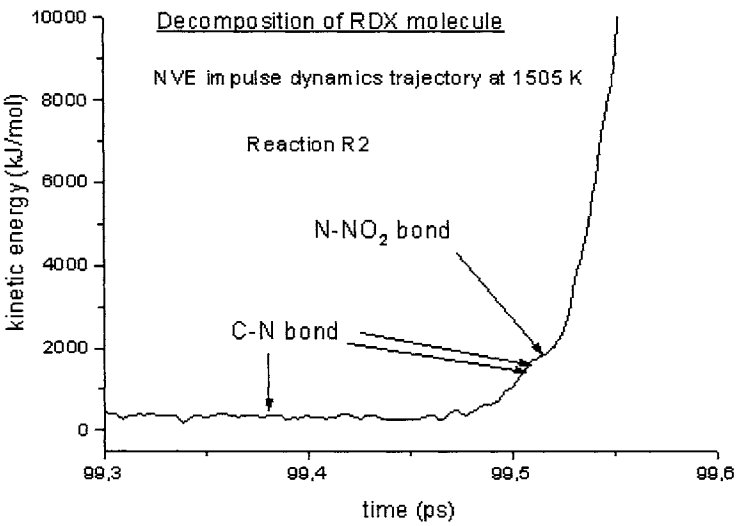

Fig. 4. Impulse dynamics trajectory for RDX, reaction R2

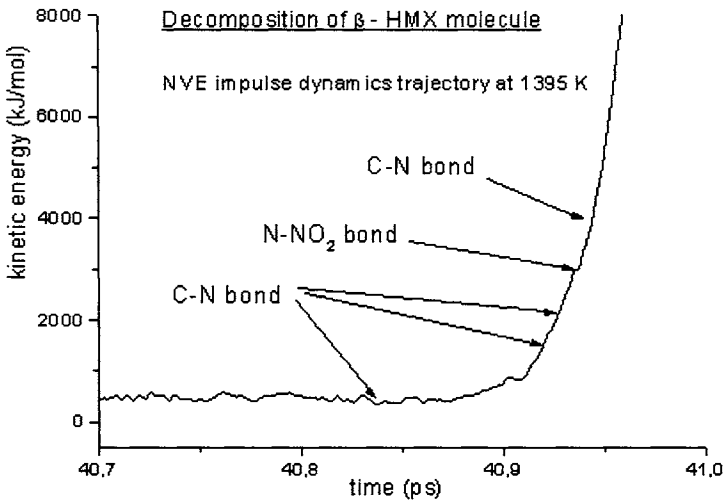

Fig. 5. Impulse dynamics trajectory for β-HMX.

3.2 Decomposition of DADNE and NQ

The course of dynamic trajectory for DADNE and NQ is very different from that for RDX and β–HMX, as one can see from the comparison of Fig. 3 – 7. The difference is in the time dependence of kinetic energy after the start of decomposition process. In case of RDX and β–HMX the kinetic energy starts to increase dramatically during the decomposition, anyway the increase is monotonous. Decomposition of DADNE and NQ starts with the rupture of N-H bond followed by the rupture of C-N bond. However in this case the decomposition is accompanied with the large fluctuations of kinetic energy, as one can see in the Fig. 6 and 7.

3.3 Parameters characterizing the decomposition process

Analysis of dynamic trajectories enabled us to determine two parameters, characterizing the decomposition process:

- $\langle E_k(NO_2) \rangle$ - as the average value of kinetic energy corresponding to the rupture of C (or N)- NO_2 bond and release of the first NO_2 group (averaging over set of dynamic trajectories)
- $\langle \Delta E_{k50} \rangle$ - as the average increment of the kinetic energy in 50 fs after the end of decomposition, which was defined as the moment when molecules is split

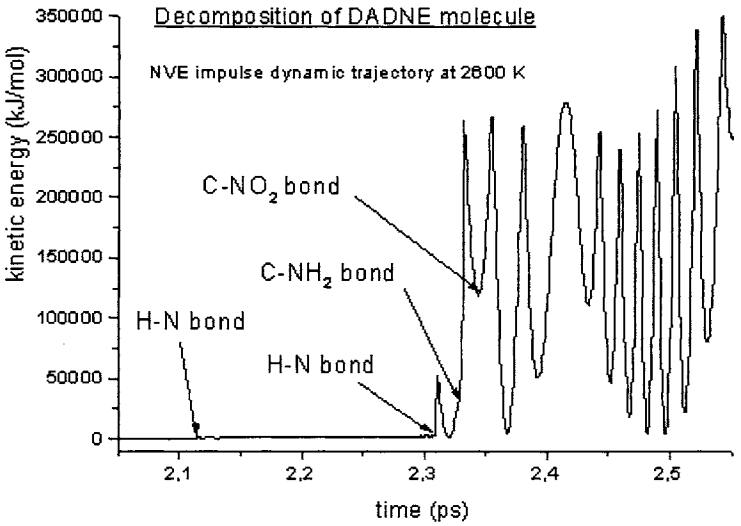

Fig. 6. Impulse dynamics trajectory for DADNE

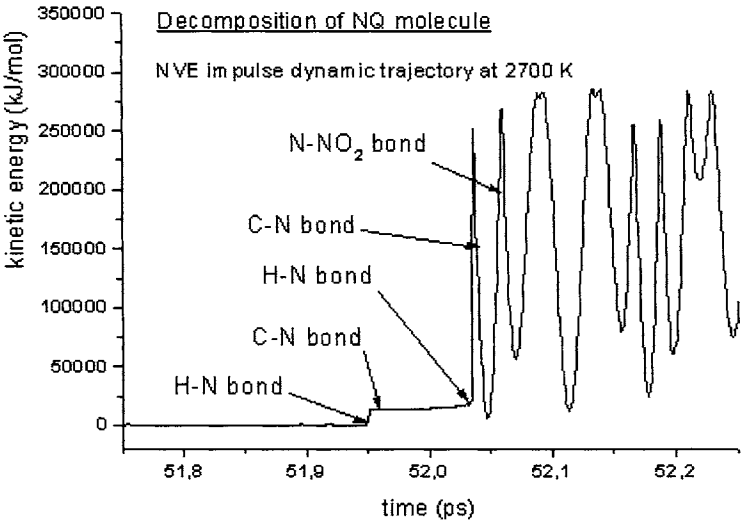

Fig. 7. Impulse dynamics trajectory for NQ.

into fragments containing 2-3 atoms. The time t(N-NO_2), when the first nitro-group is released is not convenient starting point for the estimation of $<\Delta E_{k50}>$, as it depends strongly on the reaction pathway (R1 or R2), as one can see in the Fig. 3-5.

In case of RDX and β–HMX the value of $<\Delta E_{k50}>$ characterizes reliably the slope of the monotonous E_k ~ *time* dependence immediately after the decomposition. In case of DADNE and NQ the vibrating E_k ~ *time* dependence during and after the decomposition requires a strong smoothing to catch the trend of the energy curve. Thus in this case the parameter $<\Delta E_{k50}>$ provide us only with a qualitative very rough characteristics. Calculated parameters $<E_k(NO_2)>$ and $<\Delta E_{k50}>$ are summarized in Table 1 together with the experimentally determined characteristic *h* (the critical value of the fall height of the drop weight) and calculated E_D (detonation energy) overtaken from the Ref.5.

To compare the reaction pathways R1 and R2 we analyzed dynamic trajectories for RDX corresponding to the process R1 and R2 in the Fig. 3 and 4. The parameters estimated from these two trajectories are:

- E_k *(*NO_2*)* – instantaneous value of kinetic energy corresponding to the release of the first nitro-group in the dynamics trajectory,
- E_k *(d)* – instantaneous kinetic energy corresponding to the decomposition of the molecule (splitting into fragments) at the time t_d,
- ΔE_{k50} – increment of kinetic energy per 50 fs after the t_d (time of the molecule decomposition).

These parameters are summarized in the Table 2. As one can see in Table 2, the release of the first nitro-group and the gradual rupture of C-N bonds may differ in various reaction pathways R1, R2 or in mixed R1/2 pathway. It is evident, that the instantaneous value of $E_k(NO_2)$ obtained from one dynamic trajectory only, can not be the reliable characteristics of decomposition process. On the other hand the parameters E_k *(d)* and ΔE_{k50} do not change significantly for various trajectories corresponding the same molecule and can serve as characteristics of decomposition process for a given molecule.

The comparison of calculated and experimental characteristics for all investigated molecules is in the Table 1. As one can see the $<E_k(NO_2)>$ parameters exhibit the same trend as the *h* values in dependence on the molecule type. On the other hand, the course of $<\Delta E_{k50}>$ values agrees with the course of the detonation energy E_D in dependence on the molecule type. Both calculated parameters $<E_k(NO_2)>$ and $<\Delta E_{k50}>$ obtained from the classical molecular dynamics simulations agree with the experimental characteristic *h* and calculated values of E_D in Ref. 5,16.

Table 1.
Comparison of experimental (*h*) and calculated value of E_D with characteristics of the explosive materials $<E_k(NO_2)>$, $<\Delta E_{k50}>$) obtained from dynamics trajectories; *h* - the impact sensitivity, E_D - detonation energy, $<E_k(NO_2)>$ – average kinetic energy corresponding to the release of the first nitro-group in the dynamics trajectory, $<\Delta E_{k50}>$ – average kinetic energy increment per 50 fs after the molecule decomposition.

Molecule:	h (cm)	$<E_k(NO_2)>$ (kJ/mol)	E_D (kJ/cm^3)	$<\Delta E_{k50}>$ (kJ/mol)
RDX	24	1500	8.321	24600
β–HMX	26	1700	8.858	29900
DADNE	100	119500	7.889	15000
NQ	177	190200	6.650	8200

Table 2.
Decomposition of RDX, comparison of trajectory parameters for reactions R1 and R2. Comparison of dynamic characteristics for decomposition of RDX molecule by reaction R1 and R2: E_k (NO_2) - kinetic energy corresponding to the release of the first nitro-group in the dynamics trajectory, E_k *(d)* – energy corresponding to the decomposition of the molecule (splitting into fragments), ΔE_{k50} – increment of kinetic energy per 50 fs after the molecule decomposition. Values in this table are not averaged and represent instantaneous values determined from two different trajectories illustrated in the Fig. 3 and 4.

	E_k (NO_2) (kJ/mol)	E_k (d) (kJ/mol)	ΔE_{k50} (kJ/mol)
Reaction R1	1200	1711	24900
Reaction R2	1760	1760	24300

4. CONCLUSIONS

Classical molecular dynamics simulations revealed in details the mechanism of the molecular decomposition for four selected molecules: RDX, β–HMX, DADNE and NQ. Parameters obtained from dynamic trajectories agree with the experimental characteristics *h*, describing the impact sensitivity and with calculated values of detonation energy for all investigated molecules. The parameters obtained from dynamics simulations could be used for fast effective testing of explosive materials. Anyway the method of testing based on dynamic simulations still needs to be worked out more preciously. That means:

- to extend the tests to large sets of dynamic trajectories
- to include the dynamic simulations of decomposition in crystal structure, what is very time-consuming

- to extend the tests to a larger group of explosive materials to confirm the validity of present conclusions.

Anyway, present results offered us a good chance to characterize the explosive materials by a reliable way using classical molecular dynamics simulations.

ACKNOWLEDGEMENTS:

The authors express their gratitude to the Ministry of Industry and Commerce of the Czech Republic for supporting the work within the framework of research project No. FC-M2/05 and to Grant Agency of the Czech Republic for support of an access to the crystallography database in Cambridge (within the framework of the project No. 203/02/0436).

REFERENCES:

[1] P. Politzer, J.S. Murray, J.M. Seminario, P. Lane, M.E. Grice and M.C. Concha, J. Mol. Struct. (Theochem), 573 (2001) 1.
[2] M.M. Kuklja, J. Phys. Chem. B, 105 (2001) 10159.
[3] D.V. Shalashilin and D.L. Thompson, J. Phys. Chem. A, 101 (1997) 961.
[4] Y. Kohno, K. Ueda and A. Imamura, J. Phys. Chem., 100 (1996) 4701.
[5] P. Vávra, Proc. 4th Seminar "New Trends in Research of Energetic Materials" Univ. of Pardubice, Pardubice, Czech Republic, April 2001, pp. 345-351.
[6] S. Zeman, R. Huczala and Z. Friedl, J. Energet. Mater., 20 (2002) 53.
[7] B.M. Rice, G.F. Adams, M. Page and D.L. Thompson, J. Phys. Chem., 99 (1995) 5016.
[8] C.J. Wu and L.E. Fried, Proc. 11th International Symposium on Detonation, Colorado, 1998, pp. 490-497.
[9] H. Dorsett, Computational Studies of FOX-7, a New Insensitive Explosive, DSTO Aeronautical and Maritime Research Laboratory, Salisbury South Australia, 2000, pp. 1-19.
[10] C.J. Wu and L.E. Fried, J. Phys. Chem. A, 101 (1997) 8675.
[11] *Cerius*^{2} documentation, Molecular Simulations Inc, San Diego, 2000.
[12] C.S. Choi and E. Prince, Acta Cryst. B, 28 (1972) 2857.
[13] C.S. Choi and H. P. Boutin, Acta Cryst. B, 26 (1970) 1235.
[14] U. Bemm and H. Östmark, Acta Cryst. C, 54 (1998) 1997.
[15] A.J. Bracuti, J. Chem. Crystallography, 29 (1999) 671.
[16] P. Vávra, Proc. 3rd Seminar "New Trends in Research of Energetic Materials" Univ. of Pardubice, Pardubice, Czech Republic, April 2000, pp. 223-232.
[17] A.T. Hagler, E. Huler and S. Lifson, J. Am. Chem. Soc., 96 (1974) 5319.
[18] A.K. Rappé and W.A. Goddard III, J. Phys. Chem., 95 (1991) 3358.